Three-Dimensional Dynamic Localization of Light from a Time-Dependent Effective Gauge Field for Photons

Luqi Yuan and Shanhui Fan

Department of Electrical Engineering, and Ginzton Laboratory, Stanford University, Stanford, California 94305, USA

We introduce a method to achieve the three-dimensional dynamic localization of light. We consider a dynamically modulated resonator lattice that has been previously shown to exhibit an effective gauge potential for photons. When such an effective gauge potential varies sinusoidally in time, dynamic localization of light can be achieved. Moreover, while previous works on such an effective gauge potential for photons were carried out in the regime where the rotating wave approximation is valid, the effect of dynamic localization persists even when the counterrotating term is taken into count.

The effect of dynamic localization is of fundamental importance in understanding coherent dynamics of a charged particle in a periodic potential. When such a charged particle is, in addition, subjected to a time-harmonic external electric field, the wave function of the particle can become completely localized [1,2]. This effect has been studied in a number of systems [3–13], and has been demonstrated in experiments involving a Bose-Einstein condensate or optical lattices [14,15].

Localization of a photon, especially in the full three dimensions, is of great practical and fundamental importance for the control of light [16,17]. Anderson localization [18] of light, which uses disordered but time-independent photonic structures, has been extensively explored [19–21]. Dynamic localization of light, which uses ordered but time-dependent structures, provides a significant alternative. The photon is a neutral particle; thus, there is no naturally occurring time-harmonic electric field that couples to the photon. To achieve dynamic localization of the photon, one therefore needs to synthesize an effective electric field. Up to now, extensive experimental and theoretical works have focused on light propagation in a waveguide array, where the effect of dynamic localization manifests by analogy as the cancellation of diffraction when the array is modulated in space along the propagation direction [22–27]. There has not been, however, any demonstration of a true three-dimensional localization of light in a photonic structure undergoing time-dependent modulation.

In this Letter, we show that the concept of photonic gauge potential provides a mechanism to achieve the dynamic localization of light in the full three dimensions. It has been theoretically proposed [28] and experimentally demonstrated [29–31] that when the refractive index of a photonic structure is modulated in time sinusoidally, the phase of the modulation corresponds to an effective gauge potential for photon states [32–35]. References [28–35] utilized this correspondence to create a spatially inhomogeneous, but time-invariant gauge potential distribution, in

order to study effects associated with an effective magnetic field for photons, including the photonic Aharnov-Bohm effect [28,29,31], and the photonic analogue of the integer quantum hall effect [32]. In contrast, here we create a gauge potential that is spatially homogenous or periodic, but temporally varying. We show that such a time-dependent gauge potential naturally leads to a time-varying effective electric field for photons, which can be used to create a three-dimensional dynamic localization of light. Moreover, while Refs. [28,32–35] have only considered the regime where the rotating wave approximation is valid, here we show that such dynamic localization persist even when the counterrotating term is taken into account.

We start with the same model system as discussed in detail in Refs. [32,33], consisting of either a one-dimensional or three-dimensional photonic resonator lattice as shown in Fig. 1. The lattice consists of two types of resonators (A and B) with frequencies ω_A and ω_B, respectively. The Hamiltonian of the system is

$$H = \omega_A \sum_m a_m^\dagger a_m + \omega_B \sum_n b_n^\dagger b_n$$
$$+ \sum_{\langle mn \rangle} V \cos[\Omega t + \phi_{mn}(t)](a_m^\dagger b_n + b_n^\dagger a_m), \quad (1)$$

where $V \cos[\Omega t + \phi_{mn}(t)]$ is the coupling strength between the nearest-neighbor resonators. $\Omega = \omega_A - \omega_B$. ϕ_{mn} is the phase of the coupling strength modulation. In this Letter, we will consider the situations where such a modulation phase itself is modulated in time, and refer to such modulation of the phase ϕ_{mn} as the *phase modulation*. $a^\dagger$ (a) and $b^\dagger$ (b) are the creation (annihilation) operators in the A and B sublattice, respectively.

We note that Eq. (1) can be derived from Maxwell's equations in three dimensions. The derivation is provided in the Supplemental Material [36]. The key point here is that one can construct a vectorial modal basis upon which the three-dimensional electromagnetic fields can be expanded. The dynamics of the modal expansion coefficients can then
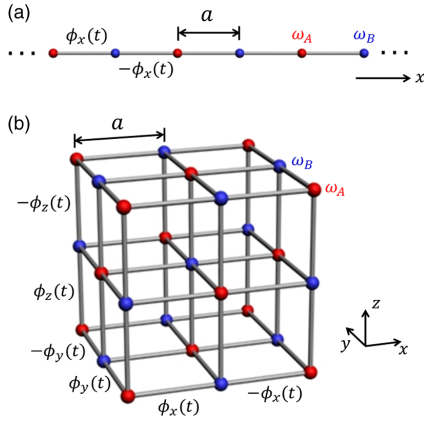
FIG. 1 (color online). A one-dimensional (a) and a three-dimensional (b) photonic resonator lattice with two kinds of resonators with frequency ω_A (red dots) and ω_B (blue dots). The nearest-neighbor coupling is dynamically modulated and the phase of the coupling constant modulation itself can be time dependent with the signs being flipped between two neighboring bonds. The lattice is assumed infinite in all directions.

be described in the form that is reminiscent of the Schrödinger equation with a tight-binding Hamiltonian, which forms the starting point of our investigation. This technique has been previously used in the literature to account for three-dimensional FDTD numerical simulations [37,41–43] and actual experiments [44].

In the limit $V \ll \Omega$, the rotating wave approximation is valid. Therefore, we can simplify the Hamiltonian and rewrite it in the rotating frame [32]

$$H = \sum_{\langle mn \rangle} \frac{V}{2} \left(e^{-i\phi_{mn}(t)} c_m^\dagger c_n + e^{i\phi_{mn}(t)} c_n^\dagger c_m \right), \quad (2)$$

where $c_{m(n)} = e^{i\omega_{A(B)}t} a_m(b_n)$. In general, such a system has a dynamic effective gauge field [32]

$$\vec{A}_{mn}^{\text{eff}} = \hat{l}_{mn} \phi_{mn}(t)/a, \quad (3)$$

where $\hat{l}_{mn}$ is a unit vector and a is the distance between two nearest-neighbor sites. Here, however, we choose the modulation phases such that in Eq. (2), all bonds along the same direction have the same phase; e.g., all bonds along the x direction have the same phase, $\phi_x(t)$. In the three-dimensional case, $\phi_y(t)$ and $\phi_z(t)$ are similarly defined. Since the phases are uniform in space, the system has zero effective magnetic field.

We now show that with a proper choice of the time dependency of these phases, we can achieve dynamic localization. As an illustration we consider the one-dimensional case in some detail. The three-dimensional case naturally follows. In the one-dimensional case, as an intuitive analysis, we can write the Hamiltonian, Eq. (2), in the wave vector space ($\boldsymbol{k}$ space)

$$H = \sum_{k_x} V c_{k_x}^\dagger c_{k_x} \cos[k_x a - \phi_x(t)]. \quad (4)$$

Hence, the system has an instantaneous photonic band structure $\omega(k_x) = V \cos[k_x a - \phi_x(t)] = V \cos[(k_x - A_x)a]$. The effect of a spatially uniform photonic gauge potential is a shift of the band structure in $\boldsymbol{k}$ space [33,35]. Since the structure maintains translational invariance, the wave vector k_x is a conserved quantity throughout the modulation process. The group velocity of the wave packet of the photon with wave vector k_x is given by

$$v_g(k_x) = \frac{\partial \omega(k_x)}{\partial k_x} = -V a \sin[k_x a - \phi_x(t)]. \quad (5)$$

At different values of ϕ_x, the group velocity at the same wave vector can have either positive or negative signs.

To demonstrate dynamic localization, we choose a phase modulation of the form $\phi_x(t) = \alpha \cos(\omega_M t)$, where α and ω_M are the amplitude and the frequency of the phase modulation, respectively. Thus, the average group velocity over one phase-modulation period $2\pi/\omega_M$ is

$$\langle v_g(k_x) \rangle = -V a \sin(k_x a) J_0(\alpha), \quad (6)$$

where J_0 is the zeroth-order Bessel function by choosing α be to a zero of J_0, the average group velocity is zero for all k_x. Thus, all wave packets of the system become localized, signifying the presence of dynamic localization. Importantly, the condition for dynamic localization here is related to the strength of the phase modulation, and is independent of the phase-modulation frequency, ω_M.

We confirm the intuitive analysis above, based on the instantaneous band structure, by a rigorous numerical calculation of the Floquet eigenstates of the Hamiltonian in Eq. (1). In this numerical analysis, we use the Hamiltonian of Eq. (4), and directly compute the quasienergy ε at each k_x, following the same procedure as in Refs. [2,45,46]. The resulting ε as a function of phase-modulation strength α, for different k_x's, are plotted in Fig. 2. At each α, the range of the values of the quasienergy indicates the bandwidth of the quasienergy band structure. The onset of the dynamic localization corresponds to the collapse of the bandwidth. In Fig. 2, we indeed observe the
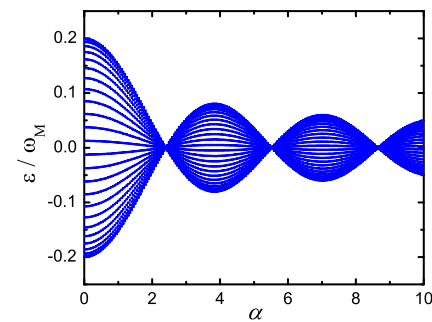

FIG. 2 (color online). The quasienergies as a function of α, for the Hamiltonian of Eq. (4), with $\phi_x(t) = \alpha \cos(\omega_M t)$. Here we choose $V = 0.2\omega_M$. Each curve corresponds to a different wave vector k_x, in the range, $-\pi/a < k_x < \pi/a$.

collapse of bandwidth when the phase-modulation strength approaches each of the zeros of J_0.

For the study of electronic dynamic localization, the effect of a time-varying electric field is typically described through the use of a spatially nonuniform *scalar* potential, as described by a Hamiltonian [1,2]

$$\tilde{H} = \sum_{\langle mn \rangle} \frac{V}{2}(c_m^\dagger c_n + c_n^\dagger c_m) - \sum_n n\alpha\omega_M \sin(\omega_M t)c_n^\dagger c_n. \quad (7)$$

In contrast, we have used a *vector* potential that is spatially periodic. Our Hamiltonian of Eq. (2) is in fact equivalent to Eq. (7) by a gauge transformation:

$$|\Psi\rangle = \sum_n v_n c_n^\dagger |0\rangle \rightarrow |\tilde{\Psi}\rangle = \sum_n \tilde{v}_n c_n^\dagger |0\rangle = \sum_n v_n e^{i\theta_n} c_n^\dagger |0\rangle, \quad (8)$$

where $|\Psi\rangle$ satisfies the Schrödinger equation, $i(\partial/\partial t)|\Psi\rangle = H|\Psi\rangle$ or $i\dot{v}_n = (V/2)[e^{-i\alpha\cos(\omega_M t)}v_{n+1} + e^{i\alpha\cos(\omega_M t)}v_{n-1}]$. With a gauge choice of $\theta_n = -n\alpha\cos(\omega_M t)$, the gauge-transformed state $|\tilde{\Psi}\rangle$ then satisfies

$$i\frac{\partial}{\partial t}|\tilde{\Psi}\rangle = \sum_n i\dot{v}_n e^{i\theta_n} c_n^\dagger |0\rangle - \sum_n v_n \dot{\theta}_n e^{i\theta_n} c_n^\dagger |0\rangle$$

$$= \frac{V}{2}\sum_n [e^{-i\alpha\cos(\omega_M t)}v_{n+1} + e^{i\alpha\cos(\omega_M t)}v_{n-1}]e^{i\theta_n} c_n^\dagger |0\rangle$$

$$- \sum_n v_n \dot{\theta}_n e^{i\theta_n} c_n^\dagger |0\rangle$$

$$= \frac{V}{2}\sum_n [v_{n+1}e^{i\theta_{n+1}} + v_{n-1}e^{i\theta_{n-1}}]c_n^\dagger |0\rangle$$

$$- \sum_n n\alpha\omega_M \sin(\omega_m t)v_n e^{i\theta_n} c_n^\dagger |0\rangle$$

$$= \tilde{H}|\tilde{\Psi}\rangle, \quad (9)$$

where $\tilde{H}$ is given in Eq. (7). Therefore, the two Hamiltonians of Eqs. (2) and (7) are indeed equivalent to each other, as they are related by a gauge transformation. A similar gauge transformation has been used in the study of waveguide array [22]. Certainly, a time-varying gauge potential for an electron is related to an electric field applied on the electron. Here, we have shown that a time-varying effective gauge potential for a photon also analogously produces an effective electric field applied on the photon.

Unlike the waveguide array approach, where the effect of photonic dynamic localization manifests through an analogy as the cancellation of diffraction in a static structure, in our approach here one can directly achieve dynamic photon localization in all three dimensions. We consider the Hamiltonian of Eq. (1) for the three-dimensional lattice as shown in Fig. 1(b). We choose the phase modulation $\phi_{x,y,z}(t) = \alpha\cos(\omega_M t)$. The intuitive derivation of dynamic localization condition [Eqs. (5)–(6)] can then be straightforwardly generalized to the full three dimensions. Full three-dimensional dynamic localization is achieved provided that the modulation strength above is chosen to be a zero of the J_0, for all choices of the phase-modulation frequency, ω_M.

Similar to the one-dimensional case, the intuitive derivations for dynamic localization for three dimensions can be confirmed by a rigorous Floquet analysis showing band collapse. Instead, here we provide the evidence of a full three-dimensional dynamic localization, by a direct simulation of photon dynamics in a $40a \times 40a \times 40a$ three-dimensional lattice. The simulation is done by solving the coupled-mode equation [34]

$$id|\Psi(t)\rangle/dt = H(t)|\Psi(t)\rangle. \quad (10)$$

Here $|\Psi\rangle = [\sum_m v_m(t)a_m^\dagger + \sum_n v_n(t)b_n^\dagger]|0\rangle$ gives the photon state with the amplitude at site $m(n)$ described by $v_{m(n)}(t)$. $H(t)$ is the time-dependent Hamiltonian of Eq. (1). The initial wave packet of the photon at $t = 0$ has the form $|\Psi(0)\rangle = \prod_{\eta=x,y,z}\exp[-(\eta-\eta_0)^2/w^2 + ik_\eta\eta]$, where (x_0, y_0, z_0) is the center of the wave packet with waist w. The results are plotted in Fig. 3. In the absence of phase modulation, Fig. 3(a) shows the initial wave packet of the photon. The wave packet propagates freely in the space with time and reaches to the corner of the lattice at $t = 1.25a/c$ [see Fig. 3(b)]. In contrast, in the presence of phase modulation with a choice of the amplitude $\alpha = 2.40483$ and frequency $\omega_M = 1.5c/a$, the wave packet of the photon is localized near its initial position throughout the entire duration of the simulation. This is demonstrated in Figs. 3(c) and 3(d), which show the wave packet's positions at $t = 1.25a/c$ and $t = 5a/c$, respectively. The simulation here provides a direct visualization of the dynamic localization process in three dimensions.

Up to this point we have used the rotating wave approximation for the Hamiltonian in Eq. (1). Previous discussions
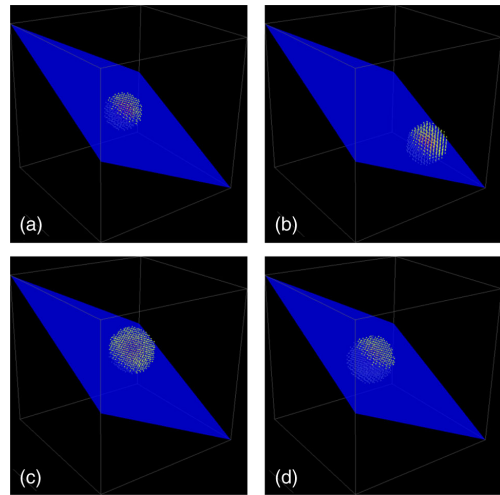

FIG. 3 (color online). Propagation of a photon wave packet in a $40a \times 40a \times 40a$ three-dimensional lattice. (a) The initial condition at $t = 0$, with $x_0 = y_0 = z_0 = 20a$ and $k_x = -k_y = -k_z = -1.283a^{-1}$. (b) The wave packet at $t = 1.25a/c$ with no phase modulation. (c) and (d) The wave packet at $t = 1.25a/c$ and $t = 5a/c$, respectively, with phase modulation. The parameters of the phase modulation are $\alpha = 2.40483$ and $\omega_M = 1.5c/a$. The coupling strength between the resonators is $V = 2.4\pi c/a$.

on the photonic gauge field in this Hamiltonian have all assumed the rotating wave approximation. On the other hand, in the experimental demonstration of the photonic gauge field one often uses electro-optic modulation of the refractive index [30]. In many electro-optic modulations, the strength of the modulation, as measured in $\delta n/n \times \omega_0$, where n is the refractive index of the structure, δn is the index change, and ω_0 is the operating frequency, can be much larger than the modulation frequency Ω on the order of a few GHz; therefore, it is important to understand the validity of the gauge potential concept beyond the rotating wave approximation. Here we show that the dynamic localization effect persists even in the regime where the rotating wave approximation is not valid.

We provide the results in one dimension. The generalization to three dimensions is straightforward. For the treatment beyond the rotating wave approximation, we again start by providing an intuitive treatment based on the instantaneous band structure. We then confirm the intuitive treatment through an exact numerical analysis of the Floquet band structure. The Hamiltonian, Eq (1), can be written in $\boldsymbol{k}$ space as

$$H = \sum_{k_x} (\omega_A a_{k_x}^\dagger a_{k_x} + \omega_B b_{k_x}^\dagger b_{k_x}) + \sum_{k_x} V a_{k_x}^\dagger b_{k_x}$$
$$\times \{e^{i\Omega t} \cos[k_x a + \phi_x(t)] + e^{-i\Omega t} \cos[k_x a - \phi_x(t)]\}$$
$$+ \text{H.c.} \tag{11}$$

Performing the transformation, $c_{k_x} = e^{i\omega_{A(B)}t} a_{k_x}(b_{k_x})$, we obtain

$$H = \sum_{k_x} V c_{k_x}^\dagger c_{k_x} \{\cos[k_x a - \phi_x(t)]$$
$$+ \cos(2\Omega t)\cos[k_x a + \phi_x(t)]\}. \tag{12}$$

We notice that the first term is the same as Eq. (4) and the second term is the counterrotating term. From Eq. (12) we can straightforwardly obtain the instantaneous band structure and hence the instantaneous group velocity at a wave vector k_x, since the Hamiltonian in the presence of the counterrotating term is still periodic in real space. Again, assuming that the modulation phase $\phi_x = \alpha \cos(\omega_M t)$, the average group velocity over one phase-modulation period $(2\pi/\omega_M)$ is

$$\langle v_g(k_x) \rangle = -Va\sin(k_x a)J_0(\alpha)$$
$$- Va\frac{\omega_M}{2\pi}\int_0^{2\pi/\omega_M} dt\cos(2\Omega t)\sin[k_x a - \alpha\cos(\omega_M t)]. \tag{13}$$

To facilitate the analytic calculation, we assume that

$$2\Omega = n\omega_M, \tag{14}$$

where n is a positive integer, and the second term in Eq. (13), denoted as $\langle v_g(k_x)\rangle_{\text{CR}}$, can be calculated analytically as

$$\langle v_g(k_x)\rangle_{\text{CR}} = Va \times \begin{cases} (-1)^{m+1}\sin(k_x a)J_n(\alpha) & n = 2m \\ (-1)^m \cos(k_x a)J_n(\alpha) & n = 2m+1. \end{cases} \tag{15}$$

By choosing $\alpha = 2.40483$, which corresponds to $J_0(\alpha) = 0$, the first term in Eq. (13) vanishes. And the correction due to

the second term can be made arbitrarily small by choosing a sufficiently large n in Eq. (14), i.e. by choosing the phase-modulation frequency to be sufficiently small as compared to the frequency of coupling strength modulation. Thus, dynamic localization can still be accomplished in the regime where rotating wave approximation no longer applies. This result can be straightforwardly generalized to three dimensions. Three-dimensional dynamic localization should occur when $2\Omega = n\omega_M$, provided that all bonds along each direction has the same phase $\phi_{x,y,z}(t) = \alpha \cos(\omega_M t)$ with the phase-modulation amplitude α being a zero of J_0.

We confirm the intuitive analysis above by calculating the Floquet band structure in the case where $V = 0.2\Omega$, and hence the rotating wave approximation is no longer valid (blue lines in Fig. 4), and by comparing such calculations to the prediction of the range of quasienergies with the rotating wave approximation (red lines in Fig. 4). Figure 4(a) shows the case with $\Omega = 2\omega_M$. Introducing the counterrotating term indeed modifies the band structure. Nevertheless, the bandwidth still collapses near a phase-modulation strength of $\alpha = 2.40483$. Thus, dynamic localization still occurs in this system beyond the rotating wave approximation. Figure 4(b) shows the case with $\Omega = 4\omega_M$. Comparing Figs. 4(a) and 4(b), we observe that the discrepancy in the band structures between the cases with or without rotating wave approximation becomes smaller as ω_M is reduced, in spite of the fact that with $V = 0.2\Omega$ we are significantly outside the regime where the rotating wave approximation is valid. This observation is consistent with the analytic results derived above based on instantaneous band structure.

Experimentally, the effective gauge field for photons has already been experimentally observed using two modulators [30]. The demonstration of the theoretical proposal here requires further integration of larger numbers of modulators.
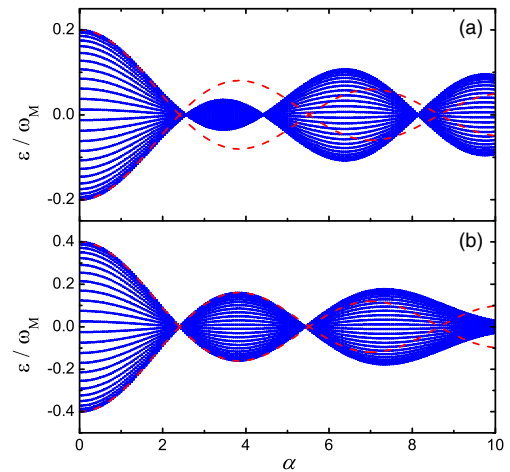

FIG. 4 (color online). Quasienergies as a function of phase-modulation strength α, for the Hamiltonian of Eq. (12), with $\phi_x(t) = \alpha \cos(\omega_M t)$. $V = 0.2\Omega$. (a) $\Omega = 2\omega_M$. (b) $\Omega = 4\omega_M$. Each blue curve corresponds to a different wave vector k_x, in the range of $-\pi/a < k_x < \pi/a$. The dashed red line is the envelope for the same Hamiltonian, but calculated using the rotating wave approximation.

The experimental feasibility of such integration has been discussed in Ref. [32]. While for illustration purpose we have focused on a photonic gauge potential through the use of temporal refractive index modulation, the concept here should be relevant for other proposals of photonic gauge potential as well, include those based on magneto-optical effects [47,48], as well as spin-dependent photonic gauge potential [49–53] and optomechnanical gauge potential [54,55]. In summary, we have shown that three-dimensional dynamic localization of light can be achieved with an effective gauge potential for photons. The results provide additional evidence of the exciting prospects of photonic gauge potential for the control of light propagation.

[1] D. H. Dunlap and V. M. Kenkre, Phys. Rev. B **34**, 3625 (1986).
[2] M. Holthaus, Phys. Rev. Lett. **69**, 351 (1992).
[3] G. Platero and R. Aguado, Phys. Rep. **395**, 1 (2004).
[4] H. N. Nazareno and Y. Lépine, Phys. Rev. B **55**, 6661(R) (1997).
[5] M. M. Dignam and C. M. de Sterke, Phys. Rev. Lett. **88**, 046806 (2002).
[6] Z. G. Wang, D. Suqing, and X. G. Zhao, Phys. Rev. B **69**, 035305 (2004).
[7] J. R. Madureira, P. A. Schulz, and M. Z. Maialle, Phys. Rev. B **70**, 033309 (2004).
[8] A. Eckardt, C. Weiss, and M. Holthaus, Phys. Rev. Lett. **95**, 260404 (2005).
[9] C. E. Creffield and G. Platero, Phys. Rev. Lett. **105**, 086804 (2010).
[10] N. Tsuji, T. Oka, P. Werner, and H. Aoki, Phys. Rev. Lett. **106**, 236401 (2011).
[11] N. Singh, Phys. Lett. A **376**, 1593 (2012).
[12] S. Longhi, J Phys Condens Matter **24**, 435601 (2012).
[13] E. N. Bulgakov and A. R. Kolovsky, Phys. Rev. B **89**, 035116 (2014).
[14] K. W. Madison, M. C. Fischer, R. B. Diener, Q. Niu, and M. G. Raizen, Phys. Rev. Lett. **81**, 5093 (1998).
[15] A. Eckardt, M. Holthaus, H. Lignier, A. Zenesini, D. Ciampini, O. Morsch, and E. Arimondo, Phys. Rev. A **79**, 013611 (2009).
[16] S. John, Phys. Rev. Lett. **58**, 2486 (1987).
[17] I. L. Garanovich, S. Longhi, A. A. Sukhorukov, and Y. S. Kivshar, Phys. Rep. **518**, 1 (2012).
[18] P. W. Anderson, Phys. Rev. **109**, 1492 (1958).
[19] T. Schwartz, G. Bartal, S. Fishman, and M. Segev, Nature (London) **446**, 52 (2007).
[20] Y. Lahini, A. Avidan, F. Pozzi, M. Sorel, R. Morandotti, D. N. Christodoulides, and Y. Silberberg, Phys. Rev. Lett. **100**, 013906 (2008).
[21] M. Segev, Y. Silberberg, and D. N. Christodoulides, Nat. Photonics **7**, 197 (2013).
[22] S. Longhi, Opt. Lett. **30**, 2137 (2005).
[23] S. Longhi, M. Marangoni, M. Lobino, R. Ramponi, P. Laporta, E. Cianci, and V. Foglietti, Phys. Rev. Lett. **96**, 243901 (2006).
[24] A. Szameit, I. L. Garanovich, M. Heinrich, A. A. Sukhorukov, F. Dreisow, T. Pertsch, S. Nolte, A. Tünnermann, and Y. S. Kivshar, Nat. Phys. **5**, 271 (2009).
[25] A. Szameit, I. L. Garanovich, M. Heinrich, A. A. Sukhorukov, F. Dreisow, T. Pertsch, S. Nolte, A. Tünnermann, S. Longhi, and Y. S. Kivshar, Phys. Rev. Lett. **104**, 223903 (2010).
[26] A. Joushaghani, R. Iyer, J. K. S. Poon, J. S. Aitchison, C. M. de Sterke, J. Wan, and M. M. Dignam, Phys. Rev. Lett. **109**, 103901 (2012).
[27] A. Crespi, G. Corrielli, G. D. Valle, R. Osellame, and S. Longhi, New J. Phys. **15**, 013012 (2013).
[28] K. Fang, Z. Yu, and S. Fan, Phys. Rev. Lett. **108**, 153901 (2012).
[29] K. Fang, Z. Yu, and S. Fan, Phys. Rev. B **87**, 060301(R) (2013).
[30] L. D. Tzuang, K. Fang, P. Nussenzveig, S. Fan, and M. Lipson, Nat. Photonics **8**, 701 (2014).
[31] E. Li, B. J. Eggleton, K. Fang, and S. Fan, Nat. Commun. **5**, 3225 (2014).
[32] K. Fang, Z. Yu, and S. Fan, Nat. Photonics **6**, 782 (2012).
[33] K. Fang and S. Fan, Phys. Rev. Lett. **111**, 203901 (2013).
[34] K. Fang, Z. Yu, and S. Fan, Opt. Express **21**, 18216 (2013).
[35] Q. Lin and S. Fan, Phys. Rev. X **4**, 031031 (2014).
[36] See Supplemental Material at http://link.aps.org/supplemental/10.1103/PhysRevLett.114.243901, which includes Refs. [32,37–40], for detailed derivation of Eq. (1) from Maxwell's equations in three dimensions.
[37] J. N. Winn, S. Fan, J. D. Joannopoulos, and E. P. Ippen, Phys. Rev. B **59**, 1551 (1999).
[38] M. P. C. Taverne, Y. D. Ho, and J. G. Rarity, J. Opt. Soc. Am. B **32**, 639 (2015).
[39] M. Qi, E. Lidorikis, P. T. Rakich, S. G. Johnson, J. D. Joannopoulos, E. P. Ippen, and H. I. Smith, Nature (London) **429**, 538 (2004).
[40] L. A. Woldering, A. P. Mosk, and W. L. Vos, Phys. Rev. B **90**, 115140 (2014).
[41] M. Reichelt and T. Meier, Opt. Lett. **34**, 2900 (2009).
[42] J. Ma, L. J. Martinez, S. Fan, and M. L. Povinelli, Opt. Express **21**, 2463 (2013).
[43] R. Novitski, B. Z. Steinberg, and J. Scheuer, Opt. Express **22**, 23153 (2014).
[44] M. Bayindir, B. Temelkuran, and E. Ozbay, Phys. Rev. Lett. **84**, 2140 (2000).
[45] J. H. Shirley, Phys. Rev. **138**, B979 (1965).
[46] H. Samba, Phys. Rev. A **7**, 2203 (1973).
[47] R. O. Umucalilar and I. Carusotto, Phys. Rev. A **84**, 043804 (2011).
[48] K. Fang and S. Fan, Phys. Rev. A **88**, 043847 (2013).
[49] M. Hafezi, E. A. Demler, M. D. Lukin, and J. M. Taylor, Nat. Phys. **7**, 907 (2011).
[50] M. Hafezi, S. Mittal, J. Fan, A. Migdall, and J. M. Taylor, Nat. Photonics **7**, 1001 (2013).
[51] A. B. Khanikaev, S. H. Mousavi, W.-K. Tse, M. Kargarian, A. H. MacDonald, and G. Shvets, Nat. Mater. **12**, 233 (2013).
[52] M. C. Rechstman, J. M. Zeuner, Y. Plotnik, Y. Lumer, D. Podolsky, F. Dreisow, S. Nolte, M. Segev, and A. Szameit, Nature (London) **496**, 196 (2013).
[53] S. Mittal, J. Fan, S. Faez, A. Migdall, J. M. Taylor, and M. Hafezi, Phys. Rev. Lett. **113**, 087403 (2014).
[54] M. Schmidt, V. Peano, and F. Marquardt, arXiv:1311.7095v2.
[55] V. Peano, C. Brendel, M. Schmidt, and F. Marquardt, arXiv:1409.5375v1.